Kinetics of a Criegee intermediate that would survive high humidity and may oxidize atmospheric SO_2

Hao-Li Huang (黃皓立)[a], Wen Chao (趙玟)[a,b], and Jim Jr-Min Lin (林志民)[a,b,1]

[a]Institute of Atomic and Molecular Sciences, Academia Sinica, Taipei 10617, Taiwan; and [b]Department of Chemistry, National Taiwan University, Taipei 10617, Taiwan

Edited by John H. Seinfeld, California Institute of Technology, Pasadena, CA, and approved July 27, 2015 (received for review July 4, 2015)

Criegee intermediates are thought to play a role in atmospheric chemistry, in particular, the oxidation of SO_2, which produces SO_3 and subsequently H_2SO_4, an important constituent of aerosols and acid rain. However, the impact of such oxidation reactions is affected by the reactions of Criegee intermediates with water vapor, because of high water concentrations in the troposphere. In this work, the kinetics of the reactions of dimethyl substituted Criegee intermediate $(CH_3)_2COO$ with water vapor and with SO_2 were directly measured via UV absorption of $(CH_3)_2COO$ under near-atmospheric conditions. The results indicate that (*i*) the water reaction with $(CH_3)_2COO$ is not fast enough ($k_{H2O} < 1.5 \times 10^{-16}$ cm^3s^{-1}) to consume atmospheric $(CH_3)_2COO$ significantly and (*ii*) $(CH_3)_2COO$ reacts with SO_2 at a near–gas-kinetic-limit rate ($k_{SO2} = 1.3 \times 10^{-10}$ cm^3s^{-1}). These observations imply a significant fraction of atmospheric $(CH_3)_2COO$ may survive under humid conditions and react with SO_2, very different from the case of the simplest Criegee intermediate CH_2OO, in which the reaction with water dimer predominates in the CH_2OO decay under typical tropospheric conditions. In addition, a significant pressure dependence was observed for the reaction of $(CH_3)_2COO$ with SO_2, suggesting the use of low pressure rate may underestimate the impact of this reaction. This work demonstrates that the reactivity of a Criegee intermediate toward water vapor strongly depends on its structure, which will influence the main decay pathways and steady-state concentrations for various Criegee intermediates in the atmosphere.

atmospheric chemistry | Criegee intermediate | SO_2 oxidation | chemical kinetics

Unsaturated hydrocarbons are emitted into the atmosphere in large quantities from either human or natural sources. Ozonolysis of unsaturated hydrocarbons produces highly reactive Criegee intermediates (CIs) (1), which may (*i*) decompose to radical species like OH radicals or (*ii*) react with a number of atmospheric species, for example, with SO_2 to form SO_3 and with NO_2 to form NO_3 (2, 3). The SO_2 oxidation by CIs has gained special attentions because the SO_3 product would be converted into H_2SO_4, an important constituent of aerosols and acid rain (4–8). For example, Mauldin et al. (4) have speculated that Criegee intermediate reactions with SO_2 may account for the discrepancy between the observed and modeled concentrations of H_2SO_4 in a boreal forest region, where various alkenes are emitted by trees.

Recently, Welz et al. (2) demonstrated an efficient method to prepare a CI in a laboratory by the reaction of iodoalkyl radical with O_2 (for example, $CH_2I + O_2 \rightarrow CH_2OO + I$). This method can produce a CI of high enough concentration that allows direct detection. With photoionization mass spectrometry (PIMS) detection, Welz et al. (2) measured the rate coefficients of the simplest CI (CH_2OO) reactions with SO_2 and NO_2. Notably, these new rate coefficients, confirmed by a few later investigations (9–11), are orders of magnitude larger than those previously used (12, 13) in atmospheric models (e.g., MCM v3.3, available at mcm.leeds.ac.uk/MCM/browse.htt?species=CH2OO), suggesting a greater role of CIs in atmospheric chemistry. This result also indicates previous ozonolysis analyses may be affected by complicated and partly unknown side reactions and may contain errors in some of the reported rate coefficients.

Typical water concentration in the troposphere (1.3×10^{17} to 8.3×10^{17} cm^{-3} at the dew point of 0–27 °C) is orders of magnitude higher than those of atmospheric trace gases like SO_2, NO_2, and volatile organic compounds (VOC) (on the order of 10^{12} cm^{-3} or less). Although it has been shown that CIs may react very fast with SO_2, NO_2, and organic acids (2, 3, 14), the reactions of CIs with atmospheric water vapor would still strongly influence the fates and concentrations of atmospheric CIs (see Fig. 1 for a simplified schematic). As expected, the reactivity of CIs toward water vapor would govern the modeling results of atmospheric H_2SO_4 formation from CIs (8, 15, 16).

However, there had been discrepancies about the reactivity of CIs toward water. Whereas studies (17–20) using C_2H_4 ozonolysis as a CH_2OO source show substantial reactivity of CH_2OO toward water vapor, despite a large scatter (10^{-17} to 10^{-12} cm^3s^{-1}) in the reported rate coefficient, other studies (2, 10, 21) using the CH_2I+O_2 reaction as a CH_2OO source reported negative observation for the CH_2OO reaction with water vapor.

More recently, Chao et al. (22) and Berndt et al. (23) investigated the reaction of CH_2OO with water vapor using the CH_2I+O_2 reaction and the C_2H_4 ozonolysis as their CH_2OO sources, respectively. Both groups observed clear second-order kinetics with respect to the concentration of water and concluded that reaction with water dimer predominates in the decay of CH_2OO under atmospheric conditions and that previous studies may require some reinterpretations. The reported rate coefficient of the CH_2OO reaction with water dimer is large, about 7×10^{-12} cm^3s^{-1} (22), leading to extremely fast decay rate of CH_2OO under typical tropospheric conditions (Table 1).

Taatjes et al. (3) and Sheps et al. (24) have reported that the *anti*-form of methyl-substituted CI (CH_3CHOO, $R^1 = H$ in Fig. 1) reacts with water vapor much faster than the *syn*- form ($R^1 = CH_3$ in Fig. 1) does. Quantum-chemical investigations (25–27) as well as studies of alkene ozonolysis (20, 28) also indicate that the structure of a CI strongly influences its reactivity toward water vapor. If one type of CI reacts slowly with water vapor but reacts quickly with

Significance

Ozonolysis of alkenes produces highly reactive Criegee intermediates. Whereas water dimer efficiently scavenges the simplest Criegee intermediate CH_2OO in the troposphere, this study clear demonstrates that water vapor does not react with dimethyl substituted Criegee intermediate $(CH_3)_2COO$, at least not fast enough to significantly consume $(CH_3)_2COO$ in the troposphere. On the other hand, $(CH_3)_2COO$ reacts with SO_2 three times faster than CH_2OO does, indicating Criegee intermediates of a structure similar to $(CH_3)_2COO$ are potential candidates for an efficient oxidant in the atmospheric SO_2 oxidation.

Author contributions: J.J.-M.L. designed research; H.-L.H. and W.C. performed research; H.-L.H. and W.C. analyzed data; and H.-L.H. and J.J.-M.L. wrote the paper.

The authors declare no conflict of interest.

This article is a PNAS Direct Submission.

[1]To whom correspondence should be addressed. Email: jimlin@gate.sinica.edu.tw.

This article contains supporting information online at www.pnas.org/lookup/suppl/doi:10.1073/pnas.1513149112/-/DCSupplemental.

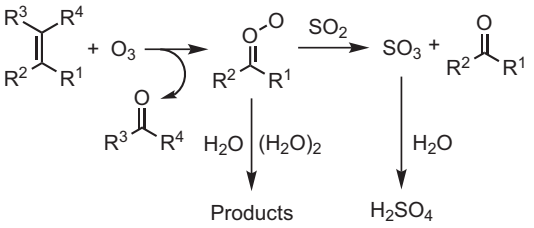

Fig. 1. Reaction scheme showing competitions for CIs between reactions with water (monomer and dimer) and with SO_2.

SO_2, these CIs may accumulate to higher concentrations and have higher probability to oxidize atmospheric SO_2. Table 1 shows selected rate coefficients for relevant CI reactions and the effective first-order decay rate coefficients (k_{eff}) of small CIs under an atmospheric condition.

As will be discussed in detail in *Discussion and Conclusions*, the steady-state concentration of a particular CI would depend on its formation rate and effective decay rate coefficient; its impact on the SO_2 oxidation would further depend on its concentration and reaction rate coefficient with SO_2. Experimental results (Table 1) show that CH_2OO and *anti*-CH_3CHOO react with water vapor very quickly (3, 22–24). Thus, their steady-state concentrations would be too low to have a significant impact in SO_2 oxidation under typical atmospheric conditions, as shown in modeling results (15, 16). On the other hand, previous experimental data for *syn*-CH_3CHOO (3, 24) are not precise enough to determine its main decay pathways in the atmosphere.

Quantum-chemistry (25–27) calculations predicted that the *anti*-form of CIs (CIs with $R^1 = H$ in Fig. 1, including CH_2OO) react with water vapor very quickly and that the *syn*- form of CIs (CIs with $R^1 \neq H$ in Fig. 1, including dialkyl-substituted CIs) react slowly with water vapor. Here, steric hindrance of the alkyl group may account for the structure dependence in the reactivity. However, due to uncertainty in the calculated rate coefficients, it is unclear about the main decay channels of the *syn*-CIs in the atmosphere. For example, some theoretical investigation (29) shows that the reactions of water vapor with *syn*-CIs may still be fast enough (with a large uncertainty) to efficiently scavenge atmospheric *syn*-CIs, whereas some other calculations (25) suggest that these reactions are too slow to consume *syn*-CIs significantly. If the latter is the case, *syn*-CIs may have higher steady-state concentrations in the troposphere and may still play an important role in the SO_2 oxidation; otherwise the steady-state concentrations of *syn*-CIs would still be low due to their fast consumption by reactions with water vapor (unless their sources are significantly larger than current estimation) and we might need to find another candidate for the unknown oxidant [oxidant X in the work by Mauldin et al. (4)] in the SO_2 atmospheric chemistry.

To shed some light on this important issue, we performed direct kinetic measurements of the reactions of dimethyl-substituted CI, $(CH_3)_2COO$, with water vapor and with SO_2 under near-atmospheric conditions. By introducing the water reactant at high concentrations, the rate coefficient of $(CH_3)_2COO$ reaction with water can be better constrained. In contrast with the fast reaction of CH_2OO with water dimer, this result shows that the relative probabilities of $(CH_3)_2COO$ reactions with SO_2 and with water vapor are comparable in the troposphere, so water alone would not completely scavenge $(CH_3)_2COO$, suggesting CIs of similar structures may play a more important role in the atmospheric oxidation of SO_2.

Results

Fig. 2*A* shows time-resolved difference absorption spectra recorded in the $(CH_3)_2CI_2/O_2$ pulsed photolysis system, in which the laser pulse defines delay time $t = 0$. The photodissociation of the $(CH_3)_2CI_2$ precursor produces $(CH_3)_2CI$ radicals; $(CH_3)_2COO$ was formed through the reaction of $(CH_3)_2CI + O_2 \rightarrow (CH_3)_2COO + I$ (30). At $t = 50$ μs, a strong absorption band peaked at 330 nm was observed, which decays with the delay time. At very long delay time (e.g., 2,000 μs), a negative difference absorption signal peaked at 296 nm was observed, which corresponds to the depletion of the $(CH_3)_2CI_2$ precursor. Fig. 2*B* shows the spectra recorded at a very similar condition but adding SO_2 gas to scavenge CIs. The absorption signal in Fig. 2*B* consists mainly of the depletion of $(CH_3)_2CI_2$ and a small amount of IO [a byproduct, likely from $I + (CH_3)_2COO \rightarrow IO + (CH_3)_2CO$]. Other possible species in the absorption cell are SO_3 and acetone, which absorb rather weakly in the studied wavelength region [the absorption cross-sections σ for the relevant species are $\sigma(SO_3) < 1 \times 10^{-21}$ cm^2, σ(acetone) $< 5 \times 10^{-20}$ cm^2, and $\sigma \sim 10^{-17}$ cm^2 for a CI] (30, 31). Following the established method of spectral analysis in similar systems (22, 31–33), the absorption band of $(CH_3)_2COO$ can be obtained from the difference between the spectra in Fig. 2 *A* and *B* and is shown in Fig. 2*C*. The resultant spectrum of $(CH_3)_2COO$ is slightly broader

Table 1. Reported bimolecular rate coefficients *k* and effective first-order rate coefficients (k_{eff} = *k*[Coreactant]) for simple CI reactions with H_2O, $(H_2O)_2$, and SO_2 at a given atmospheric condition

CI	Coreactant	[Coreactant]/cm^{-3}	*k*/cm^{3}s^{-1}	k_{eff}/s^{-1}	Reference
CH_2OO	H_2O	5.4×10^{17}	$<1.5 \times 10^{-15}$	<810	(22)
	$(H_2O)_2$	6.0×10^{14}	6.5×10^{-12}	3,900	(22)
	SO_2	1.2×10^{12}	3.9×10^{-11}	47	(2)
anti-CH_3CHOO	H_2O	5.4×10^{17}	1.0×10^{-14}	5,400	(3)
			2.4×10^{-14}	13,000	(24)
	SO_2	1.2×10^{12}	6.7×10^{-11}	80	(3)
			2.2×10^{-10}	260	(24)
syn-CH_3CHOO	H_2O	5.4×10^{17}	$<4 \times 10^{-15}$	<2,200	(3)
			$<2 \times 10^{-16}$	<110	(24)
	SO_2	1.2×10^{12}	2.4×10^{-11}	29	(3)
			2.9×10^{-11}	35	(24)
$(CH_3)_2COO$	H_2O	5.4×10^{17}	$<1.5 \times 10^{-16}$*	<81*	This work
	$(H_2O)_2$	6.0×10^{14}	$<1.3 \times 10^{-13}$*	<78*	This work
	SO_2	1.2×10^{12}	1.3×10^{-10}	160	This work

The assumed concentrations of H_2O and SO_2 correspond to a relative humidity RH = 70% and a SO_2 mixing ratio of 50 ppb at 298 K and 1 atm. Only data from direct kinetic measurements are selected.

*The rate constant of the H_2O reaction with $(CH_3)_2COO$ is obtained by assuming the rate constant of the $(H_2O)_2$ reaction with $(CH_3)_2COO$ is zero and vice versa (*SI Appendix*, Table S2); thus, these two effective decay rates should not be added together.

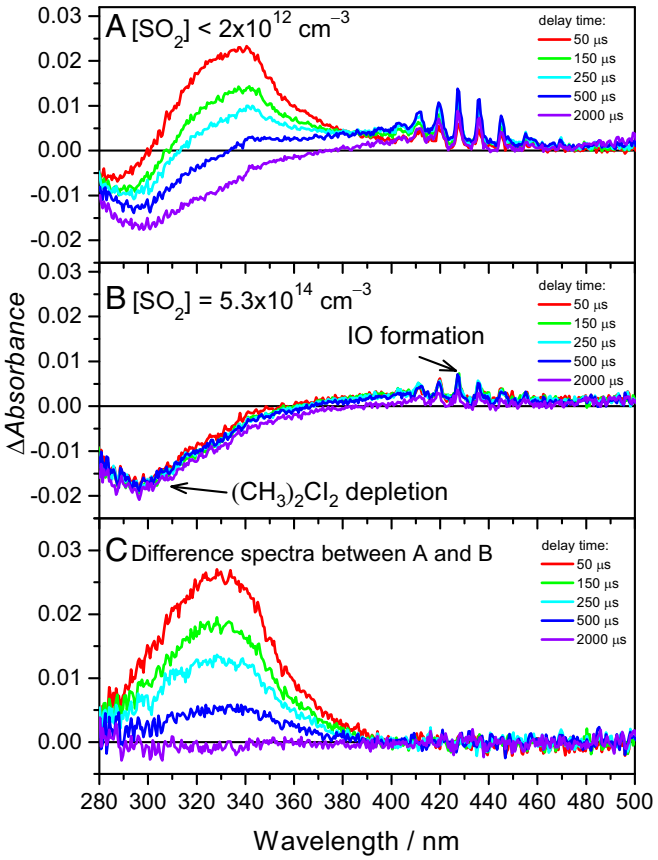

Fig. 2. Typical transient absorption spectra recorded in the $(CH_3)_2CI_2/O_2$ photolysis system at selected delay times after the photolysis laser pulse (t = 0). Total pressure was 100.1 torr (P_{N2} = 89.9 torr, P_{O2} = 10.2 torr, $[(CH_3)_2CI_2]_0 = 1.1 \times 10^{14}$ cm^{-3}). (*A*) Spectra recorded without adding SO_2. (*B*) Spectra recorded at $[SO_2] = 5.3 \times 10^{14}$ cm^{-3}; $(CH_3)_2COO$ was consumed by its reaction with SO_2. (*C*) Difference spectra between the two sets of spectra in *A* and *B*. The main spectral carrier is assigned to $(CH_3)_2COO$ because the reaction of $(CH_3)_2COO$ with SO_2 is fast. The residue contributions of the IO byproduct and the $(CH_3)_2CI_2$ precursor are minor and have been removed in *C*.

than but still consistent with the jet-cooled spectrum reported by Liu et al. (30). See *SI Appendix*, Fig. S2.

In the kinetic measurements, we chose a detection window of 335–345 nm to monitor the change in $(CH_3)_2COO$ concentrations. In this detection window, the absorption signal of IO is negligible [$\sigma(IO) = 2.7 \times 10^{-19}$ cm^2 << $\sigma((CH_3)_2COO) \sim 10^{-17}$ cm^2] (22); the absorption of the precursor $(CH_3)_2CI_2$ is small but not negligible. Fortunately, Fig. 2*B* shows that the depletion of the precursor is a constant after the photolysis laser pulse, which would not affect our kinetic analysis for $(CH_3)_2COO$.

Representative difference transient absorption traces recorded at various SO_2 concentrations are shown in Fig. 3; a more complete set of the experimental data can be found in *SI Appendix*, Figs. S3–S6 and Table S1. As mentioned above, $(CH_3)_2COO$ is the main spectral carrier for the absorption at 340 nm. The rapid rise of the signal after the photolysis laser pulse was due to $(CH_3)_2COO$ formation. When SO_2 is added, the reaction of $(CH_3)_2COO$ with SO_2 dominates in the observed decay of $(CH_3)_2COO$. When no SO_2 is added, the $(CH_3)_2COO$ decay is due mainly to reactions of $(CH_3)_2COO$ with radical species, including I atoms, OH radicals [possibly from decomposition of $(CH_3)_2COO$ (30)], and $(CH_3)_2COO$ itself, similar to the case of CH_2OO (33). Because the concentration of $(CH_3)_2COO$ in our experiment was low (on the order of 10^{11} cm^{-3}), the self-reaction between two $(CH_3)_2COO$ molecules did not dominate in the decay of $(CH_3)_2COO$, leading to the observed first-order–like decay.

The decay of the $(CH_3)_2COO$ signals can be well described by Eqs. **1** and **2**. Under the high O_2 pressure (~10 torr) used in this study, the formation time of $(CH_3)_2COO$ is within 1 μs. This formation time is relatively short in comparison with the decay time of $(CH_3)_2COO$. Thus, the fitting for the decay typically started at t = 10 μs to decouple the formation kinetics.

$$[(CH_3)_2COO] = [(CH_3)_2COO]_0 e^{-k't}, \quad [1]$$

$$-\frac{d[(CH_3)_2COO]}{dt} = k'[(CH_3)_2COO] = (k_0 + k_{SO2}[SO_2])[(CH_3)_2COO]. \quad [2]$$

Fig. 4 shows the observed pseudo–first-order rate coefficient ($k' - k_0$) as a function of SO_2 concentration, where the k_0 term (Eq. **2**) accounts for the $(CH_3)_2COO$ decay when no SO_2 was added (see *SI Appendix*, Table S1 for the values of k_0). A linear relationship between k' and $[SO_2]$ is found with the slope corresponding to the rate coefficient k_{SO2} for the $(CH_3)_2COO$ reaction with SO_2. In Fig. 4, it is obvious that the slope is different at different total pressure.

Fig. 5 plots the reaction rate coefficient k_{SO2} as a function of the total pressure with N_2 as the buffer gas. At pressure higher than 100 torr ([M] = 3.2×10^{18} cm^{-3}), the rate coefficient is leveled. This high-pressure-limit rate coefficient is 1.3×10^{-10} cm^{3}s^{-1}, about 3 times the reported rate coefficient of CH_2OO reaction with SO_2 [$k_{CH2OO+SO2} = (3.9 \pm 0.7) \times 10^{-11}$ cm^{3}s^{-1}] (2). At low pressure, the rate coefficient drops. A simple model in Fig. 6 is used to analyze the experimental data.

Quantum-chemistry studies (29) suggested that CI reaction with SO_2 would first go through a barrierless formation of a cyclic intermediate, INT* (R1). In addition, because the formation of the cyclic intermediate is quite exothermic, its stabilization requires collision with a third body (R2). Furthermore, the energized intermediate INT* may dissociate back to the reactants or form products directly (likely SO_3 + carbonyl); (R4) connects the stabilized intermediate INT to the final products.

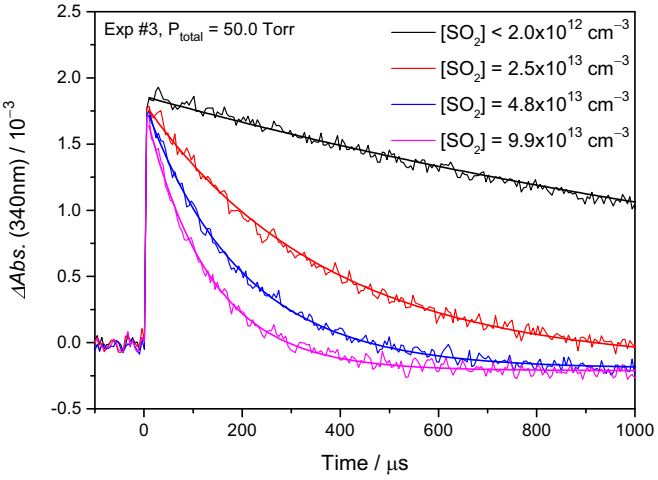

Fig. 3. Typical temporal profiles of the absorbance change at 340 nm. The change in absorbance was mainly due to $(CH_3)_2COO$ and was monitored in real time with a balanced photodiode detector at various SO_2 concentrations. The smooth lines are single exponential fit to the data.

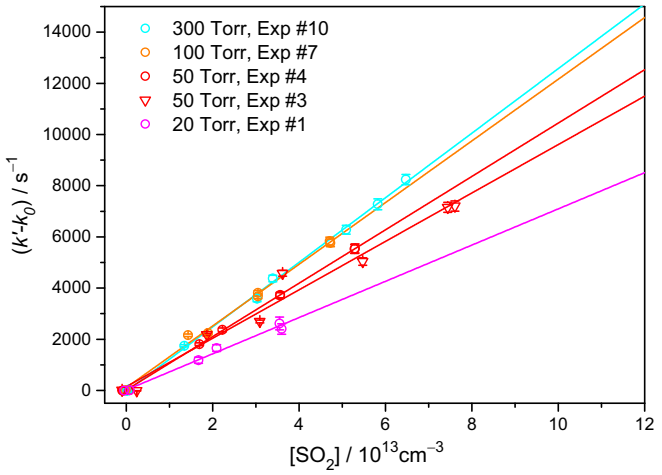

Fig. 4. Pseudo–first-order rate coefficient of $(CH_3)_2COO$ reaction with SO_2 plotted as a function of $[SO_2]$. k_0 is the rate coefficient at zero $[SO_2]$. The measurements were performed at 298 K with N_2 as the buffer gas at the indicated total pressure. The error bars indicate the SDs; the number of independent data can be found in *SI Appendix*, Table S1 for each experiment. Solid lines are linear fit to the data at the corresponding pressure. Data at higher and lower pressure ranges are shown in *SI Appendix*, Figs. S7 and S8.

Applying steady-state approximation to INT* leads to the following:

$$-\frac{d[\mathrm{CI}]}{dt}=k_1[\mathrm{CI}][SO_2]-k_{-1}[\mathrm{INT}^*]=k_{SO2}[\mathrm{CI}][SO_2], \quad [3]$$

$$k_{SO2}=\frac{k_1(k_3+k_2[M])}{k_{-1}+k_3+k_2[M]}. \quad [4]$$

Theoretical analysis (29) suggests that (R2) is the main pathway (97%) for the $(CH_3)_2COO$ reaction with SO_2 under atmospheric pressure. Thus, we may simplify the mechanism by assuming $k_2[M] >> k_3$, unless the pressure is low. (R4) may be a slow reaction, but if there are no other competing processes, the yield of R4 may still be high, as indicated by previous ozonolysis studies (20, 28, 34).

The best fit of Eq. **4** to the data of Fig. 5 is shown as the red line (the best fit gives k_3 =0). At the high-pressure limit, $k_{SO2}=k_1=1.32\times10^{-10}$ cm^3s^{-1}. Nonzero k_3 leads to a nonzero low-pressure-limit rate constant $k_1k_3/(k_{-1}+k_3)$ but a value larger than 6×10^{-11} cm^3s^{-1} for this term cannot fit the data satisfactorily (green line in Fig. 5). The error in k_1 mostly comes from the uncertainty in the absolute concentrations of SO_2, which is less than 10%. Thus, we report $k_1=(1.32\pm0.13)\times10^{-10}$ cm^3s^{-1}.

To further elucidate the role of the buffer gas, we changed the buffer gas from N_2 to CO_2 or Ne and performed similar experiments at 50 torr. *SI Appendix*, Fig. S9 shows that CO_2 is a more efficient collider than N_2 and Ne is a less efficient collider, as one may expect. Furthermore, we also investigated the pressure effect in the reaction of CH_2OO with SO_2. However, the reaction rate coefficient of CH_2OO with SO_2 does not exhibit significant pressure dependence (see *SI Appendix*, Figs. S13–S15 and Table S3 and ref. 10).

The pressure dependence of the reaction of $(CH_3)_2COO$ with SO_2 has implications in atmospheric chemistry. Applying low-pressure rates in a model may underestimate the impact of the $(CH_3)_2COO$ reaction with SO_2. Similarly, the pressure dependence of the reactions of SO_2 with other CIs needs to be investigated because quite a number of rate coefficients of CI reactions are measured under low-pressure conditions [~4 torr for PIMS experiments (2, 3, 14)].

The kinetics of the $(CH_3)_2COO$ reaction with water vapor were also measured. In sharp contrast with the fast reaction of CH_2OO with water vapor, the decay of $(CH_3)_2COO$ barely depends on $[H_2O]$, even for high water concentration up to 7×10^{17} cm^{-3} (RH = 90% at 298 K). Fig. 7 shows the first-order rate coefficients k' of $(CH_3)_2COO$ decay as a function of $[H_2O]$. We have varied the experimental conditions including the total pressure, precursor concentration, photolysis laser power, etc. (*SI Appendix*, Table S2) and the results show that the effect of water in the decay of $(CH_3)_2COO$ is extremely weak. More detailed analysis indicates the decay rate coefficient of $(CH_3)_2COO$ depends mainly on the radical concentration (*SI Appendix*, Fig. S12). We estimate an upper limit of 1.5×10^{-16} cm^3s^{-1} for the rate coefficient of the $(CH_3)_2COO$ reaction with H_2O, based on the fluctuation of the experimental data (*SI Appendix*, Table S2).

Discussion and Conclusions

So far, there is no method available to detect the concentration of any CI in the atmosphere. The estimation of the CI concentration can only be done by knowing its formation rate and consumption rate. The impact of a given CI (e.g., to the SO_2 oxidation) depends on its concentration and the rate coefficient of its reaction with SO_2, as shown in the following (Eqs. **5**–**9**):

$$\mathrm{O_3}+\mathrm{alkene}\rightarrow\mathrm{CI}\quad k_{\mathrm{form}}, \quad [5]$$

$$\mathrm{CI}\rightarrow\mathrm{Products}\quad k_{\mathrm{decay}}, \quad [6]$$

$$[\mathrm{CI}]_{ss}=\frac{k_{\mathrm{form}}[\mathrm{O_3}][\mathrm{alkene}]}{k_{\mathrm{decay}}}, \quad [7]$$

$$k_{\mathrm{decay}}=k_{\mathrm{therm}}+k_{\mathrm{H2O}}[\mathrm{H_2O}]+k_{\mathrm{w2}}[(\mathrm{H_2O})_2]+k_{\mathrm{SO2}}[SO_2]+k_{\mathrm{NO2}}[\mathrm{NO_2}]+\ldots, \quad [8]$$

$$\frac{d[SO_2]}{dt}=-k_{SO2}[\mathrm{CI}]_{ss}[SO_2]=-k_{SO2}\frac{k_{\mathrm{form}}[\mathrm{O_3}][\mathrm{alkene}]}{k_{\mathrm{decay}}}[SO_2], \quad [9]$$

where $[\mathrm{CI}]_{ss}$ is the steady-state concentration of the CI; k_{form} is the formation rate constant of the CI from its precursors (e.g., ozone

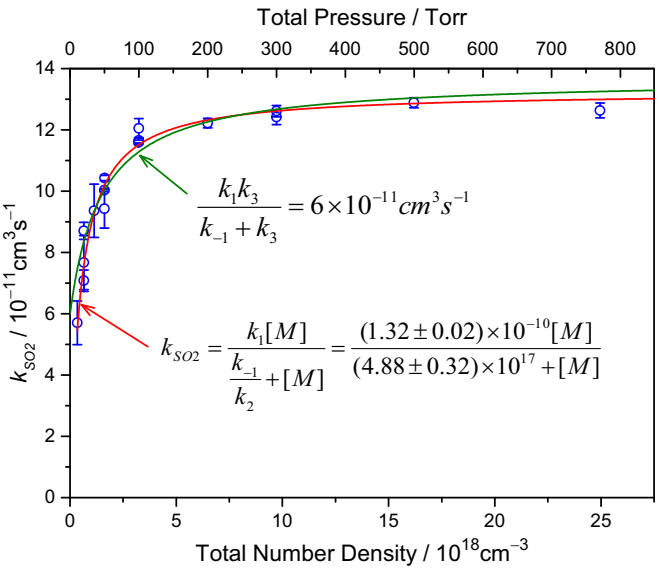

Fig. 5. Observed second-order rate coefficient of $(CH_3)_2COO$ reaction with SO_2 plotted as a function of the total pressure and number density. The fitting is plotted as solid lines. The error bars of the data indicate the SDs. The errors in the fitted equation are the SDs resulting from the fitting only, not including any possible systematic uncertainty yet. There are 18 independent measurements.

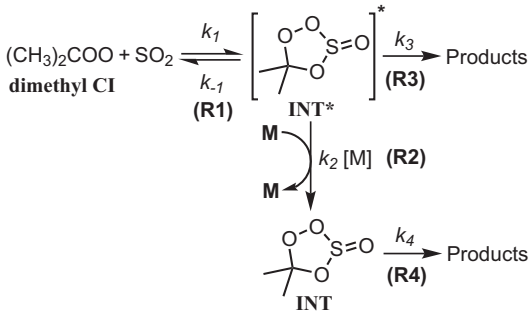

Fig. 6. Proposed mechanism for CI reaction with SO_2.

and an alkene); k_{decay} would be the summation of the effective decay rate constants k_{eff} of all possible decay pathways; k_{therm} is the thermal decomposition rate coefficient; k_{H2O}, k_{w2}, k_{SO2}, and k_{NO2} are the bimolecular rate coefficients of CI reactions with H_2O, $(H_2O)_2$, SO_2, and NO_2, respectively. The k_{therm} for $(CH_3)_2COO$ has been reported recently to be 3 ± 0.4 s^{-1} at 293 K (34) with a significant temperature dependence (28).

Considering the possible concentrations of H_2O and SO_2 in the troposphere, we can evaluate the effective decay rate constants of simple CIs by water reaction and by SO_2 reaction. As shown in Table 1, the consumptions of CH_2OO and *anti*-CH_3CHOO by water (including monomer and dimer) are extremely fast, $>10^3$ s^{-1}, predominating in their k_{decay}. The very large k_{decay} would result in very low steady-state concentrations for these CIs, limiting their roles in oxidizing other atmospheric species like SO_2 and NO_2 (see Eqs. **7**–**9**).

On the other hand, the reaction of $(CH_3)_2COO$ with H_2O is much slower, such that the water reaction would not limit the $(CH_3)_2COO$ concentration in the troposphere anymore. In addition, the rate coefficient of $(CH_3)_2COO$ reaction with SO_2 is larger than those of other known CI reactions with SO_2, indicating a greater role of $(CH_3)_2COO$ in the atmospheric SO_2 oxidation. In other words, there is a strong structure dependence in the CI oxidation of SO_2. For $(CH_3)_2COO$, its k_{decay} is smaller and its k_{SO2} is larger, such that the SO_2 oxidation rate by $(CH_3)_2COO$ is faster in comparison with those for CH_2OO and *anti*-CH_3CHOO, assuming similar formation rates (see Eq. **9**). In addition, for a CI with small k_{H2O} and k_{w2}, its k_{therm} would be another important factor that also influences its $[CI]_{ss}$ and oxidation capacity. A related issue is that the thermal decomposition of *syn*-CIs [including $(CH_3)_2COO$] may form OH radicals through a 1,4 H-migration process (30), which may be an important non-photolytic OH source in the troposphere. Again, structure dependence of k_{therm} for various CIs would need further investigation.

Previous studies of ozonolysis of 2,3-dimethyl-2-butene (tetramethyl ethylene, $R^1 = R^2 = R^3 = R^4 = CH_3$) (20, 28, 34) have provided some information about the $(CH_3)_2COO$ reactions with H_2O and with SO_2. But, the results are far from consistency. First, the reported k_{SO2} are on the order of 10^{-13} cm^3s^{-1} (34), much smaller than the value determined from the direct kinetic measurement (Table 1). A similar situation also happens for smaller CIs like CH_2OO and CH_3CHOO (12, 13, 35), suggesting there might be some systematic issues in the ozonolysis experiments. Very recently, Newland et al. (20) measured the removal of SO_2 in the presence of alkene–ozone systems and concluded that the SO_2 removal displays a clear dependence on relative humidity for all four alkene ozonolysis systems [ethene (to form CH_2OO), *cis*-2-butene (to form CH_3CHOO), *trans*-2-butene (to form CH_3CHOO), and 2,3-dimethyl-2-butene (to form $(CH_3)_2COO$)], confirming a significant reaction for stabilized CIs with H_2O. However, Berndt et al. (28) investigated the H_2SO_4 formation as a function of $[H_2O]$ in similar ozonolysis reactions and reported quite different values. The results for $(CH_3)_2COO$ are summarized in Table 2. The result by Newland et al. is not consistent with the results of Berndt et al. and this work. The reason for this discrepancy may originate from the complexity of the ozonolysis experiments, in which it is difficult to fully quantify the side reactions during the long reaction time.

It is important to note that the reactivity of a particular CI toward water vapor strongly depends on its structure. Table 1 indicates that a methyl group substitution for R^1 may alter the rate coefficient by orders of magnitude. Although ozonolysis experiments (20, 28, 34) have also shown a trend for the structure dependence, the magnitude of the reactivity difference is much smaller than what is observed in the direct kinetic measurements (Table 1). In addition, the ozonolysis experiments cannot distinguish the *anti*- and *syn*- conformers of CIs, which have quite different reactivity.

The results summarized in Table 1 give direct evidence that the reaction of water with $(CH_3)_2COO$ is greatly hindered by the methyl group at the R^1 position. Interestingly, methyl substitution seems to enhance the reactivity of CIs toward SO_2. One can imagine that CIs with more complicated substitution groups may also react with water slowly but react with SO_2 quickly, similar to $(CH_3)_2COO$. Such CIs may be the candidate for the oxidant X in the SO_2 oxidation, an important issue raised recently (4).

Considering that much of the VOC emissions consist of a large variety of alkenes, ranging from simple alkenes like C_2H_4 and C_3H_6 to bigger alkenes like isoprene, monoterpenes, sesquiterpenes, etc., various CIs are expected to form in the atmospheric ozonolysis reactions. To assess the impact of the CI+SO_2 reaction class on the atmosphere, it is critical to know the atmospheric concentration of CIs. As mentioned above, it requires the relevant rate coefficients to estimate the atmospheric concentration of a CI. Water is the third most abundant molecule in the air. The reactions of CIs with water are crucial in determining the concentrations and fate of the CIs. The slow rates of water reactions with $(CH_3)_2COO$ or with similar CIs are very difficult to measure, but very important in estimating the concentrations of those CIs and thus the oxidizing capacity of the atmosphere.

Materials and Methods

The experimental setup has been described in detail elsewhere (22, 32). In brief, $(CH_3)_2COO$ was generated from photolysis of a gaseous mixture consisting of $(CH_3)_2CI_2$, O_2, and buffer gas (N_2) at 248 nm (KrF excimer laser) via the established preparation method: $(CH_3)_2CI_2 + h\nu \rightarrow (CH_3)_2CI + I$; $(CH_3)_2CI + O_2 \rightarrow (CH_3)_2COO + I$ (2, 30). $(CH_3)_2COO$ was monitored via its strong UV absorption (30). Continuous probe light went through the photolysis reactor (25 or 20 mm inner diameter, 76 cm long) six or eight times to enhance the absorption signal.

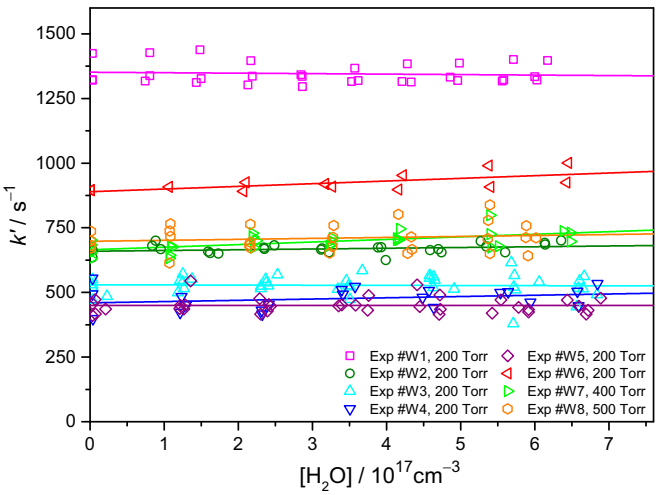

Fig. 7. Pseudo–first-order rate coefficient of $(CH_3)_2COO$ as a function of $[H_2O]$. Solid lines are linear fit to the data of each experiment. There are 223 data points (see *SI Appendix*, Table S2 for the experimental conditions).

Table 2. Ratio of the rate coefficients of $(CH_3)_2COO$ reactions with H_2O and with SO_2, k_{H2O}/k_{SO2}

k_{H2O}/k_{SO2}	Method	Reference
$<1.2 \times 10^{-6}$	Absolute direct kinetic measurements of $(CH_3)_2COO$	This work
$<4 \times 10^{-6}$	Relative measurements of the H_2SO_4 product	Berndt et al. (28)
$(8.7 \pm 2.5) \times 10^{-5}$	Relative measurements of the SO_2 and O_3 consumptions	Newland et al. (20)

Spectral Measurements. Transient absorption spectra of the reaction system were measured with a continuous broadband light source (Energetiq, EQ-99) and a time-gated iCCD spectrometer (Andor, SR303i and DH320T-18F-03). The light source was projected to the entrance of the absorption cell by an achromatic lens (Thorlabs ACA254-100-UV). To enhance the absorption signal, the probe light was reflected eight times through the photolysis reactor by a spherical mirror ($R = 1$ m, Thorlabs, CM750-500-F01) and a SiO_2 prism. The probe beam and the photolysis beam were overlapped collinearly in the photolysis reactor. For the iCCD measurement, the reference spectrum was recorded 200 μs before the photolysis pulse. Transient spectra at delay times 50, 100, 150, 200, 250, 300, 500, 1,000, and 2,000 μs were recorded.

Kinetics Measurements. Absorption signal at 340 nm was measured in real time by using a balanced photodiode detector (Thorlabs, PDB450A) and a bandpass filter (Edmund Optics, 65129, 10-nm OD4 band pass filter) and the same light source. A time-dependent transmittance change (<1%) was observed after the photolysis pulse even without adding any sample. This background did not depend on $[H_2O]$, or on $[SO_2]$. It can be subtracted by performing a background run under the same experimental condition except adding $(CH_3)_2Cl_2$. The presented data are after the background subtraction.

$[SO_2]$ Measurements. The SO_2 concentration was adjusted by controlling the amount of SO_2 in buffer gas with mass flow controllers (Brooks, 5850E or 5800E) and monitored by its UV absorption (190–330 nm) with a D_2 lamp (Ocean Optics, D-2000) and a spectrometer (Ocean Optics, Maya2000 Pro).

Relative Humidity Measurements. The relative humidity was adjusted by controlling the mixing ratio of dry and moisturized buffer gases with mass flow controllers (Brooks, 5850E or 5800E) and monitored with a humidity sensor (Rotronic, HC2-S). The temperature for measuring the water reaction was controlled at 298.2 ± 0.5 K.

Precursor Preparation. The precursor, $(CH_3)_2CI_2$, was synthesized following a reported method (36). In brief, acetone was added to hydrazine monohydrate (80 °C, >1 h) to obtain acetone hydrazone $(CH_3)_2C{=}NNH_2$. Saturated solution of iodine in ethyl ether was added to acetone hydrazone (at room temperature), which is mixed with ethyl ether and triethylamine, to obtain the final product. The structure of the synthesized $(CH_3)_2CI_2$ was checked with H-NMR spectroscopy [$(CH_3)_2CI_2$: 3.00 ppm (6H, s, Me) in $CDCl_3$] (37).

ACKNOWLEDGMENTS. The authors thank Prof. Jim-Min Fang, Ms. Ling-Wei Li, and Ms. Che-Hsuan Chang for help in organic synthesis and NMR measurement; Ms. Liang-Chun Lin and Mr. Chun-Hung Chang for help in experiments; and Prof. Yuan-Tseh Lee for discussion. This work was supported by Academia Sinica and Ministry of Science and Technology, MOST 103-2113-M-001-019-MY3, Taiwan.

1. Criegee R (1975) Mechanism of ozonolysis. *Angew Chem Int Ed Engl* 14(11):745–752.
2. Welz O, et al. (2012) Direct kinetic measurements of Criegee intermediate (CH_2OO) formed by reaction of CH_2I with O_2. *Science* 335(6065):204–207.
3. Taatjes CA, et al. (2013) Direct measurements of conformer-dependent reactivity of the Criegee intermediate CH_3CHOO. *Science* 340(6129):177–180.
4. Mauldin RL, 3rd, et al. (2012) A new atmospherically relevant oxidant of sulphur dioxide. *Nature* 488(7410):193–196.
5. Boy M, et al. (2013) Oxidation of SO_2 by stabilized Criegee intermediate (sCI) radicals as a crucial source for atmospheric sulfuric acid concentrations. *Atmos Chem Phys* 13(7):3865–3879.
6. Ehn M, et al. (2014) A large source of low-volatility secondary organic aerosol. *Nature* 506(7489):476–479.
7. Berresheim H, et al. (2014) Missing SO_2 oxidant in the coastal atmosphere?–observations from high-resolution measurements of OH and atmospheric sulfur compounds. *Atmos Chem Phys* 14(22):12209–12223.
8. Sarwar G, et al. (2014) Impact of sulfur dioxide oxidation by stabilized Criegee intermediate on sulfate. *Atmos Environ* 85(3):204–214.
9. Sheps L (2013) Absolute ultraviolet absorption spectrum of a Criegee intermediate CH_2OO. *J Phys Chem Lett* 4(24):4201–4205.
10. Stone D, Blitz M, Daubney L, Howes NU, Seakins P (2014) Kinetics of CH_2OO reactions with SO_2, NO_2, NO, H_2O and CH_3CHO as a function of pressure. *Phys Chem Chem Phys* 16(3):1139–1149.
11. Liu Y, Bayes KD, Sander SP (2014) Measuring rate constants for reactions of the simplest Criegee intermediate (CH_2OO) by monitoring the OH radical. *J Phys Chem A* 118(4):741–747.
12. Hatakeyama S, Akimoto H (1994) Reactions of Criegee intermediates in the gas phase. *Res Chem Intermed* 20(3-5):503–524.
13. Johnson D, Marston G (2008) The gas-phase ozonolysis of unsaturated volatile organic compounds in the troposphere. *Chem Soc Rev* 37(4):699–716.
14. Welz O, et al. (2014) Rate coefficients of C1 and C2 Criegee intermediate reactions with formic and acetic acid near the collision limit: Direct kinetics measurements and atmospheric implications. *Angew Chem Int Ed Engl* 53(18):4547–4550.
15. Sarwar G, et al. (2013) Potential impacts of two SO_2 oxidation pathways on regional sulfate concentrations: Aqueous-phase oxidation by NO_2 and gas-phase oxidation by stabilized Criegee intermediates. *Atmos Environ* 68:186–197.
16. Li J, Ying Q, Yi B, Yang P (2013) Role of stabilized Criegee intermediates in the formation of atmospheric sulfate in eastern United States. *Atmos Environ* 79:442–447.
17. Suto M, Manzanares ER, Lee LC (1985) Detection of sulfuric acid aerosols by ultraviolet scattering. *Environ Sci Technol* 19(9):815–820.
18. Becker K, Bechara J, Brockmann K (1993) Studies on the formation of H_2O_2 in the ozonolysis of alkenes. *Atmos Environ* 27(1):57–61.
19. Leather K, et al. (2012) Acid-yield measurements of the gas-phase ozonolysis of ethene as a function of humidity using chemical ionisation mass spectrometry (CIMS). *Atmos Chem Phys* 12(1):469–479.
20. Newland MJ, et al. (2015) Kinetics of stabilised Criegee intermediates derived from alkene ozonolysis: Reactions with SO_2, H_2O and decomposition under boundary layer conditions. *Phys Chem Chem Phys* 17(6):4076–4088.
21. Ouyang B, McLeod MW, Jones RL, Bloss WJ (2013) NO_3 radical production from the reaction between the Criegee intermediate CH_2OO and NO_2. *Phys Chem Chem Phys* 15(40):17070–17075.
22. Chao W, Hsieh J-T, Chang C-H, Lin JJ-M (2015) Atmospheric chemistry. Direct kinetic measurement of the reaction of the simplest Criegee intermediate with water vapor. *Science* 347(6223):751–754.
23. Berndt T, et al. (2014) Competing atmospheric reactions of CH_2OO with SO_2 and water vapour. *Phys Chem Chem Phys* 16(36):19130–19136.
24. Sheps L, Scully AM, Au K (2014) UV absorption probing of the conformer-dependent reactivity of a Criegee intermediate CH_3CHOO. *Phys Chem Chem Phys* 16(48):26701–26706.
25. Ryzhkov AB, Ariya PA (2004) A theoretical study of the reactions of parent and substituted Criegee intermediates with water and the water dimer. *Phys Chem Chem Phys* 6(21):5042–5050.
26. Kuwata KT, Hermes MR, Carlson MJ, Zogg CK (2010) Computational studies of the isomerization and hydration reactions of acetaldehyde oxide and methyl vinyl carbonyl oxide. *J Phys Chem A* 114(34):9192–9204.
27. Anglada JM, González J, Torrent-Sucarrat M (2011) Effects of the substituents on the reactivity of carbonyl oxides. A theoretical study on the reaction of substituted carbonyl oxides with water. *Phys Chem Chem Phys* 13(28):13034–13045.
28. Berndt T, et al. (2014) H_2SO_4 formation from the gas-phase reaction of stabilized Criegee intermediates with SO_2: Influence of water vapour content and temperature. *Atmos Environ* 89:603–612.
29. Vereecken L, Harder H, Novelli A (2012) The reaction of Criegee intermediates with NO, RO_2, and SO_2, and their fate in the atmosphere. *Phys Chem Chem Phys* 14(42):14682–14695.
30. Liu F, Beames JM, Green AM, Lester MI (2014) UV spectroscopic characterization of dimethyl- and ethyl-substituted carbonyl oxides. *J Phys Chem A* 118(12):2298–2306.
31. Ting W-L, Chen Y-H, Chao W, Smith MC, Lin JJ (2014) The UV absorption spectrum of the simplest Criegee intermediate CH_2OO. *Phys Chem Chem Phys* 16(22):10438–10443.
32. Smith MC, et al. (2014) UV absorption spectrum of the C2 Criegee intermediate CH_3CHOO. *J Chem Phys* 141(7):074302.
33. Ting W-L, et al. (2014) Detailed mechanism of the $CH_2I + O_2$ reaction: Yield and self-reaction of the simplest Criegee intermediate CH_2OO. *J Chem Phys* 141(10):104308.
34. Berndt T, et al. (2012) Gas-Phase ozonolysis of selected olefins: The yield of stabilized Criegee intermediate and the reactivity toward SO_2. *J Phys Chem Lett* 3(19):2892–2896.
35. Jenkin ME, et al. (2015) The MCM v3.3 degradation scheme for isoprene. *Atmos Chem Phys Discuss* 15:9709–9766.
36. Pross A, Sternhell S (1970) Oxidation of hydrazones with iodine in the presence of base. *Aust J Chem* 23(5):989–1003.
37. Karabatsos G, Osborne C (1968) Structural studies by nuclear magnetic resonance—XVI: Conformations and configurations of hydrazones. *Tetrahedron* 24(8):3361–3368.